

Designing a Self-Associated Cationic Polymer for Enhanced Compatibility, Palatability, and Gastric Release of Cefuroxime Axetil

Anupa R. Menjoge and Mohan G. Kulkarni*

Polymer Science and Engineering Division, National Chemical Laboratory, Pune 411008, India

Received July 12, 2006; Revised Manuscript Received November 1, 2006

Cefuroxime axetil (CA) has exhibited interactions with the polymers hydroxypropyl methylcellulose phthalate, cellulose acetate trimellitate, and Eudragit E resulting in the generation of unacceptable amounts of impurities and degradation. Formulations, which mask the bitter taste of CA and release it immediately in the stomach, have therefore not been possible. In an attempt to overcome the interaction with CA, we report a self-associated cationic polymer (NREP) containing methyl methacrylate (MMA), 2-hydroxy ethylmethacrylate (HEMA), and 4-vinyl pyridine (4-VP). The hydrogen bonding between the pyridine nitrogen and the hydroxyl groups of HEMA results in strong intrachain associations, prevents interactions between NREP and CA, and inhibits degradation of CA. This has been validated by differential scanning calorimetry, Fourier transform infrared spectroscopy, NMR, and high-performance liquid chromatography analysis. These self-associations restrict polymer chain motions, enhance biocompatibility, and lead to a higher T_g , which ensures that NREP does not become tacky in processes involving heat. The judicious choice of the hydrophobic and hydrophilic monomers renders the polymer hydrophobic enough as to mask the bitter taste of CA at near neutral pH. Incorporation of the basic monomer 4-VP ensures rapid dissolution of the polymer and release of CA at the acidic pH prevalent in the stomach. The work indicates an approach to design pH-sensitive polymers for dosage forms that meet the pharmacokinetic requirements of the drug.

Introduction

Excipients form an integral part of all pharmaceutical dosage forms. Drugs exhibit poor solubility and stability, and the role of excipients is to provide physical and chemical stability and retain bioavailability. A major consideration in the choice of biomaterials for drug delivery is drug–polymer interaction, drug transformation, and its degradation.¹ At times excipients also promote the degradation of drugs. Functional groups or residues in excipients are prone to interaction with certain drugs. These interactions often modify the physicochemical characteristics of the drug.² The interactions are either reversible or irreversible in nature and alter in most cases dissolution, bioavailability, safety, and efficacy and in extreme cases even the stability of the drug.^{3–5} Acetyl salicylic acid is degraded by magnesium stearate forming salicylic acid, salisalicylic acid, and acetyl salisalicylic acid.^{6,7}

A wide range of excipients has been used for temporal and spatial release of drugs by the oral route. In addition, to release the drugs at the desired site, excipients are used to help deliver drugs to patients in forms that facilitate administration. Pediatric and geriatric patients often experience difficulty in swallowing tablets and capsules. Drugs are therefore administered to such patients as solutions, suspensions, and emulsions. This often leads to the perception of bitterness^{8,9} and patient noncompliance.^{9,10} The choice of the taste-masking technique to overcome this problem is governed by the physicochemical and pharmacokinetic parameters of the drug and the type of dosage form.

Cefuroxime axetil (CA) is a second-generation cephalosporin antibiotic administered orally and is known to have an extremely bitter taste.¹¹ Extensive efforts have been made in the past to

develop oral suspensions based on CA. Cellulose acetate trimellitate (CAT), hydroxypropyl methylcellulose phthalate (HPMCP), Eudragit E (EE), and Eudragit L (EL) have been evaluated as possible excipients to encapsulate the drug.^{12,13} Lorenzo-Lamosa et al.¹³ reported that the CA–EE microspheres exhibited the desired release profile, but the drug was degraded in the presence of the polymer. Also in the presence of CAT, the degradation of CA led to unacceptably high proportions of impurities.¹²

Donn et al.¹⁴ studied the bioavailability of CA from tablets and suspensions based on wax-coated CA granules and concluded that the tablets and suspensions were not bioequivalent. The lower bioavailability of CA from suspension than that from the tablet was attributed to the wax coating on the CA granules. The wax coating causes relatively delayed release of CA as the release takes place only on forming the stearate salt in alkaline pH due to the interaction between sodium ions and stearic acid.¹¹ Dantzig et al.¹⁵ showed that CA is hydrolyzed to cefuroxime in the intestinal lumen by the enzyme esterases. This conversion of CA to cefuroxime in the intestine results in reduced absorption and low bioavailability in humans.¹⁶ Similar findings were reported by Campbell et al.¹⁶ and Ruiz-Balaguer et al.¹⁷ These reports imply that excipients such as wax coatings and enteric polymers that release the drug in the intestine are not ideal carriers for this drug. CA has a low oral bioavailability of 37–52%,^{18,19} and hence any further reduction in the bioavailability due to inappropriate choice of excipient should be avoided.

The physicochemical properties of CA constrain the options of excipients for formulation. CA has a limited absorption window restricted to the upper gastric region. In addition CA has a tendency to gel in the presence of moisture at physiological temperatures (37 °C) leading to poor dissolution and reduced absorption.²⁰ The physicochemical and pharmacokinetic properties of this difficult to formulate drug warrant the use of

* Author to whom correspondence should be addressed. Phone: +91-20-25902178. Fax: +91-20-25902618. E-mail: mg.kulkarni@ncl.res.in.

Table 1. NREP Characteristics

	composition (%)		MW ^a	PI ^b	T _g (°C)
	feed	by NMR			
MMA	60	62	58 550	1.6	121.2
HEMA	25	27			
VP	15	11			

^a Molecular weight. ^b Polydispersity index.

hydrophobic polymer coating, releasing it in the gastric region without inactivation. Further, the polymer should be capable of taste-masking CA. Development of such a polymer has not been reported to our knowledge.

To overcome the above limitations in the formulation of CA, we report the design, synthesis, and physicochemical characteristics of the cationic terpolymer (NREP). We investigated the interaction between CA and the basic monomers 4-vinylpyridine (4-VP) and dimethylaminoethyl methacrylate (DMAEMA) by HPLC and selected 4-VP, as CA was stable in its presence. To enhance the stability of CA further, proton donating and accepting groups were incorporated in NREP to ensure the self-association within the polymer. We used methyl methacrylate (MMA) and 2-hydroxyethyl methacrylate (HEMA) as hydrophobic and hydrophilic monomers, respectively, along with 4-VP.

The rapid dissolution at pH 1.2 and hydrophobicity of NREP were optimized by the judicious choice of the monomers and the composition. Before undertaking the formulation optimization, a detailed investigation of physicochemical interactions between NREP and CA was undertaken using differential scanning calorimetry (DSC), Fourier transform infrared (FTIR) spectroscopy, NMR, and high-performance liquid chromatography (HPLC). The results indicate that CA is stable in the presence of NREP. The encapsulation of CA in NREP releases CA immediately at gastric pH and masks its bitter taste at the pH of saliva. Results of in vitro and in vivo biological reactivity tests indicate that the polymer is nontoxic.²¹

Experimental Section

Materials. Methyl methacrylate (MMA), 2-hydroxy ethyl methacrylate (HEMA), 4-vinylpyridine (4-VP), and dimethylamino ethyl methacrylate (DMAEMA) were purchased from Sigma-Aldrich. Tetrahydrofuran for chromatography was purchased from Merck. Azobisisobutyronitrile (AIBN) was obtained from local suppliers. Cefuroxime axetil (CA) and its reference standard were gifts of Lupin Laboratories Ltd. Deuterated chloroform (CDCl₃) and acetone-*d*₆ for NMR were purchased from Sigma-Aldrich. Ammonium dihydrogen phosphate and acetanilide (HPLC grade) were purchased from Fluka. All other chemicals were analytical grade, and solvents were purchased from Qualigens.

Synthesis of the pH-Sensitive Polymer. The pH-sensitive polymers were synthesized as disclosed by us earlier.^{22,23} The trace impurity of ethylene glycol dimethacrylate (EGDMA) was removed from HEMA before polymerization to yield the soluble polymer. Freshly distilled monomers MMA and 4-VP were used for polymerization. Typically for the synthesis of polymer P9, referred to as NREP (Table 1), 18.72 g of MMA (0.186 mol), 11.58 g of HEMA (0.088 mol), and 5.07 g of 4-VP (0.048 mol) were added to 80 mL of dimethyl formamide in a 250 mL round-bottom flask. Solution polymerization of the monomer mixture was carried out using AIBN as an initiator at 65 °C for 18 h. The polymer solution was concentrated on a rotary evaporator. The polymer was dissolved in a (1:1) dichloromethane/methanol mixture and precipitated in water to remove unreacted monomers. Polymers were dried at 27 °C under vacuum for 72 h.

Table 2. Composition of CA Microspheres

formulation ^a	CA/NREP	loading efficiency	CA loading
	ratio	(%)	(%)
F1	1:5	90.0	15.0
F2	1:3	89.2	22.3
F3	1:2	89.4	29.8
F4	1:1	88.4	44.2

^a Formulations containing 900 mg of CA.

Fabrication of the Polymer film. Films of thicknesses of 0.06–0.07 mm were cast by spreading 12% w/v polymer solution in chloroform on a Teflon surface with an area of 19.64 cm² (Supporting Information).

pH-Dependent Dissolution/Swelling. Polymer films (10 mm × 15 mm) were exposed to 15 mL of water and buffers of pH 1.2, 4.5, and 5.8. At pH 1.2 the polymer films were observed for the dissolution over 10, 15, 30, 45, and 60 min. The films were exposed to water, pH 4.5 and 5.8, for 7 days, and their equilibrium swelling was calculated (for details, see the Supporting Information).

In Vitro and In Vivo Biological Reactivity Test. The biological reactivity of NREP was evaluated as per standard tests described in the United States Pharmacopeia²¹ (USP) (for details, see the Supporting Information).

Physicochemical Characterization of Interactions between CA and NREP. The physical mixture of CA with NREP (1:1 w/w) was prepared by mixing the two thoroughly in a mortar and pestle. The CA–NREP blend (1:1 w/w) was prepared by adding CA to a 5% w/v NREP solution in dichloromethane/methanol (1:2). The blend was collected after evaporation of the solvent and used for further investigations. The physicochemical characterization of the physical mixture and blend was carried out by DSC, X-ray diffraction (XRD), FTIR, NMR, and HPLC analysis. For instrumentation details, see the Supporting Information.

Encapsulation of CA by NREP. The NREP solution was prepared in a mixture of methanol/dichloromethane (2:1). CA was added to the NREP solution under magnetic stirring, and this mixture was dispersed slowly in light liquid paraffin containing 0.25% Span 85 using a mechanical stirrer. The stirring was continued for 3–4 h at 500 rpm. The microspheres were separated by filtration and washed with petroleum ether to remove the paraffin oil. The microspheres so formed were dried under vacuum for 24 h at room temperature. The composition of the microspheres is shown in Table 2.

Determination of CA Content. CA microspheres (50 mg) were dissolved in 2 mL of methanol and sonicated for 5 min. The volume was made to 50 mL using 0.07 N HCl. The solution was filtered and diluted further for the analysis. CA content was determined at 278 nm using a Shimadzu UV160 IPC UV–vis spectrophotometer. Each sample was analyzed in triplicate.

CA Release from Microspheres. Microspheres containing cefuroxime equivalent to 125 mg were placed in a basket containing 900 mL of 0.07 N HCl. The dissolution was carried out in an Electrolab USP type II apparatus at 75 rpm at 37 ± 0.5 °C. The samples were collected after 30, 60, 90, 120, 180, and 240 min. The amount of CA released was estimated at 278 nm using the Shimadzu UV spectrophotometer. The dissolution tests were done in triplicate.

Gustatory Test/Taste Evaluation. The microspheres equivalent to four doses of cefuroxime (125 mg × 4) were suspended in syrup (85% w/w sucrose) of pH 4.4 adjusted by addition of sodium citrate and citric acid buffer. The taste evaluation of the reconstituted suspension was performed for 7 days. Each day few drops of the reconstituted suspension were placed on tongue of four volunteers for 10–20 s and then spat out. The bitterness level was recorded. The volunteers were asked to grade the sample each day on a numerical scale of 0–4 with the score “0” for sweet taste, “1” for acceptable, “2” for acceptable but slightly bitter, “3” for bitter, and “4” for very bitter taste.

Scanning Electron Microscopy. Quanta SEM Series, FEI Company, environmental mode was used to record morphological changes

occurring in situ in microspheres on exposure to the dissolution medium of 0.07 N HCl. The microspheres were introduced into the Quanta specimen chamber, and 0.07 N HCl was introduced until the microspheres were immersed completely. Changes occurring in individual microspheres were recorded by introduction of drops of 0.07 N HCl onto the microsphere for a span of 10 min. The acid medium was removed from the sample holder by applying vacuum.

The integrity of the NREP coat on microspheres at pH 4.5 and 5.8 was also examined. The samples were prepared by immersing the microspheres in buffer pH 4.5 and 5.8 for a period of 7 days. The wet samples were filtered and mounted immediately in the sample holder and examined for surface modifications of the microspheres.

Results and Discussion

The aim of the study was to design a cationic polymer that does not deactivate CA due to drug–polymer interactions, releases it rapidly in the stomach, and has taste-masking ability. The following sections describe how the cationic terpolymer NREP meets the requirements of an ideal reverse enteric polymer along with biocompatibility and without adverse interactions with CA. Reverse enteric polymers are soluble in gastric pH (acidic) and insoluble at neutral and near neutral pH.

Screening Criteria for Polymers. The reverse enteric polymer for taste-masking of granules for an oral suspension should exhibit immediate drug release at the gastric pH. Yet the drug release should be negligible at the pH of saliva (>5.8). The leaching of the drug from polymer-coated granules should be low in aqueous media (liquid oral formulations for pediatric patients) to avoid the perception of bitterness.

The drug release from the polymer depends upon the relative rates of sorption and diffusion of the penetrant and the diffusion of the drug. In the case of the drug encapsulated in a cationic polymer, two conditions have to be met: (1) The aqueous reconstitution medium should not penetrate the polymer so that the release of the drug is inhibited. A hydrophobic/glassy polymer will ensure this. (2) At the gastric pH, the medium should penetrate the polymer and cause rapid dissolution of the polymer without appreciable swelling. This will ensure that the drug does not undergo polymorphic transformation/gelation, which inhibits its release resulting in lower bioavailability. This rapid dissolution without appreciable swelling of the polymer is crucial for CA formulations.

Sorption of liquids into glassy polymers results in either bulk scale changes or case II transport. In the former case quasi-equilibrium swelling is followed by a slow approach to final true equilibrium. Polymers, which undergo bulk scale changes, will obviously not be suitable for drugs such as CA that tend to gel in the presence of moisture. If the sorption of the penetrant medium follows case II transport and the swollen layer undergoes rapid dissolution, then the drug immobilized in the glassy polymer region will be protected, while that in the swollen layer will be released as a result of dissolution.

Apart from pH-dependent behavior, the polymer should not become tacky during processes involving heat such as drying and heat-sealing; hence a high T_g is also desirable. All of the above parameters influenced the selection criteria for monomers in the terpolymer. The copolymer composition was optimized to achieve this end result.

Monomer Choice for the Reverse Enteric Polymer. Polymers containing cationic groups are soluble in an acidic medium. The basic monomer DMAEMA was found to interact with CA causing its inactivation as seen from the HPLC analysis (Figure S4, Supporting Information). We chose 4-VP as the cationic monomer, which has a lower pK_a , viz. 5.45–5.65,^{24,25}

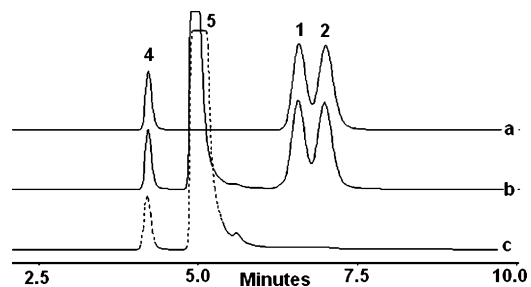


Figure 1. Chromatograms of (a) CA, (b) CA–4VP mixture, and (c) internal standard 4-VP: (1) isomer B; (2) isomer A; (3) cefuroxime not generated; (4) internal standard acetanilide; (5) 4-VP.

than that of DMAEMA (pK_a 8.4).²⁶ The ionization of poly-(vinyl pyridine) is almost zero at pH 4.^{27,28} Strong association between the pyridine nitrogen and the hydroxyls in a blend of homopolymers poly(vinyl pyridine) and poly(HEMA) is reported by Cesteros et al.²⁹ We chose to incorporate HEMA along with 4-VP in the terpolymer so that the intrachain self-association would suppress the interaction of the pyridine nitrogen with CA. These assumptions were validated by detailed investigation of physicochemical interactions between CA and NREP. To impart the hydrophobic character we incorporated MMA as the hydrophobic monomer. Since HEMA increased the hydrophilicity of the polymer, the composition had to be optimized to achieve the desired pH-dependent dissolution behavior.

The monomer structure, charge density, molecular weight, and nature of the amine group affect the cytotoxicity, and all of these factors were considered in the design of NREP. One of the criteria for the selection of the basic monomer was the influence of the structure of the monomers on the cytotoxicity. 4-VP was chosen as the basic monomer since it is a tertiary amine and it has been reported in the past that the toxicity of tertiary amines is lower as compared to those of the primary and secondary amines.^{30–32}

The low pK_a of 4-VP is also responsible for the lower cytotoxicity as it suppresses ionization at physiological pH. The ionization of the polymer is related to the pK_a value of the functional monomer, which in turn influences charge density on the polymer. Hence NREP would also exhibit lower toxicity. The charge density on the polymer is considered a key parameter that enhances interactions with the cell membrane, thus causing cell damage. Polymers with a higher charge density are more cytotoxic.^{33,34} The NMR analysis revealed that the incorporation of 4-VP is 11%, which is low, contributing to a low charge density.

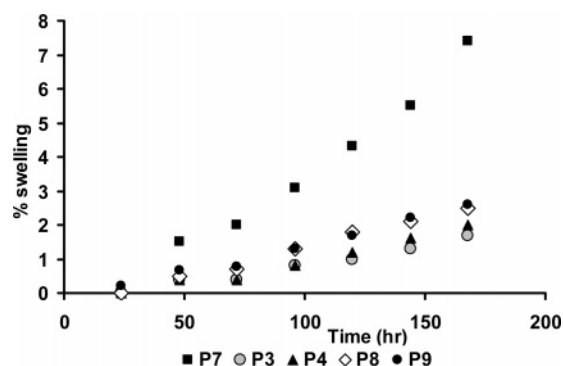
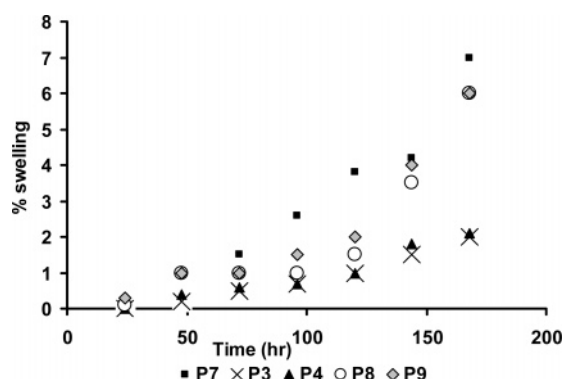
Apart from charge density, the polymer chain flexibility affects the binding with cell membranes. The FTIR study revealed that pyridine nitrogen and hydroxyls from HEMA in NREP are associated. This is also reflected in the higher T_g of NREP over the weight average value. The polymer chain mobility in NREP is restricted by self-association. Hence NREP was expected to elicit a lower biological response, if any. The in vitro and in vivo biocompatibility studies support these assumptions.

Evaluation of Interaction between CA and the Basic Monomer. The stability of CA in the presence of 4-VP was investigated prior to the synthesis of the terpolymer. CA and 4-VP were taken in 1:1 w/w ratio in methanol. This solution was analyzed by HPLC after 5–10 min. The peak for 4-VP appeared at 4.9 min, and the peaks corresponding to diastereomers A and B of CA were also seen (Figure 1). The cefuroxime content was 0.34%, which was the same as that observed in

Table 3. Polymer Compositions and Their pH Responses

polymer	MMA/HEMA/4-VP % w/w (by NMR)	dissolution time (min)		
		pH 1.2	pH 4.5	pH 5.8
P1	83:0:17	up to 60 ^a	soluble, day 2 ^c	soluble, day 4 ^c
P2	61:21:18	up to 30 ^b	soluble, day 4 ^c	soluble, day 4 ^c
P3	69:20:11	up to 45 ^a	insoluble, low swelling ^b	insoluble, low swelling ^b
P4	68:23:9	up to 45 ^a	insoluble, low swelling ^b	insoluble, low swelling ^b
P5	52:37:11	up to 15 ^b	soluble, day 4 ^c	soluble, day 4 ^c
P6	56:32:12	up to 15 ^b	soluble, day 4 ^c	soluble, day 4 ^c
P7	61:30:9	up to 15 ^b	insoluble, high swelling ^c	insoluble, high swelling ^c
P8	65:24:11	up to 15–30 ^b	insoluble, low swelling ^b	insoluble, low swelling ^b
P9	62:27:11	up to 15–30 ^b	insoluble, low swelling ^b	insoluble, low swelling ^b

^a Slow dissolution. ^b Acceptable behavior. ^c Solubility/swelling not desired.

**Figure 2.** Swelling behavior of polymer films exposed to a buffer at pH 4.5.**Figure 3.** Swelling behavior of polymer films exposed to a buffer at pH 5.8.

the working standard of CA (see HPLC method validation in the Supporting Information). The Δ -2 isomer was not seen. The resolution between the two diastereomers was 1.67, and the ratio $rA/(rA + rB)$ was 0.52. The total impurities generated are below 3%. This indicates that CA is stable in presence of the 4-VP monomer. These results imply that CA would be stable in the presence of NREP where the nitrogen of 4-VP is bound with hydroxyls of HEMA.

Polymer Composition Optimization. Various polymer compositions were synthesized and screened for swelling and dissolution behavior by exposing the polymer films to buffers of pH 1.2, 4.5, and 5.8. The monomer composition in the polymer was optimized (see compositions P1–P9 in Table 3) based on the observed response at different pH values. CA was found to be stable in presence of 4-VP; hence all polymers were synthesized using 4-VP as the basic monomer. The response of these polymers at buffer pH values of 4.5 and 5.8 is shown in Figures 2 and 3, respectively. The dissolution rate of the polymer films at pH 1.2 is shown in Table 3. A copolymer of

MMA and 4-VP containing 95% w/w of MMA in the feed was synthesized. At pH 1.2, the copolymer did not solubilize even after 4–5 h because of the high MMA content. The resulting polymer was glassy and hydrophobic, and the penetration of the buffer medium in the polymer film was very slow. To enhance the rate of penetration of the buffer and also the rate of dissolution, a copolymer (P1) containing 83% MMA and 17% 4-VP was synthesized.

On exposure to a buffer at pH 1.2, the copolymer film (P1) became translucent with gradual dissolution. Under acidic conditions this copolymer swelled in the buffer more rapidly because of higher 4-VP content. The swelling of the film led to the formation of a glassy core and a swollen outer shell. As time proceeded the glassy core receded inward, while the swollen shell dissolved. Thus the overall thickness of the film decreased with time leading eventually to the complete dissolution of the film after 60 min. On exposure to a buffer at pH 4.5, the film dissolved after 24 h, and at pH 5.8 it showed water uptake followed by dissolution after 3 days. The increase in 4-VP content enhanced the rate of dissolution of the polymer film at pH 1.2 but also led to the dissolution of the polymer at pH 5.8. Such a polymer would be of little use as a reverse enteric polymer for oral suspension. Another concern in increasing the content of the basic monomer 4-VP was the possibility of interaction with CA. There was a need to enhance the rate of polymer dissolution at acidic pH without increasing the content of the basic monomer.

To enhance the rate of penetration of the buffer at pH 1.2 without enhancing the rate of dissolution/swelling at pH 5.8, incorporation of the neutral hydrophilic monomer HEMA was considered. The association of the hydroxyl groups of HEMA with the pyridine nitrogen is reported. Introduction of HEMA would serve to (a) enhance the dissolution and (b) provide self-associations within the polymer avoiding its interaction with CA. A series of terpolymers P2–P9 were synthesized and evaluated to ensure rapid dissolution at acidic pH and minimal swelling at pH 4.5 and above.

The terpolymer P2 containing 61%, 21%, and 18% w/w of MMA, HEMA, and 4-VP, respectively, was synthesized. In composition P2, the content of MMA was lowered, and that of 4-VP was unaltered as compared to that of P1. The incorporation of HEMA resulted in rapid and complete dissolution of P2 at pH 1.2 in 30 min as compared to 60 min for P1. However the presence of the hydrophilic component HEMA resulted in dissolution of the polymer at pH 4.5 and 5.8 after 2–3 days (Table 3). To impart hydrophobic character to the polymer, compositions P3 and P4 were synthesized in which the content of MMA was increased (69% and 68% w/w) and the content

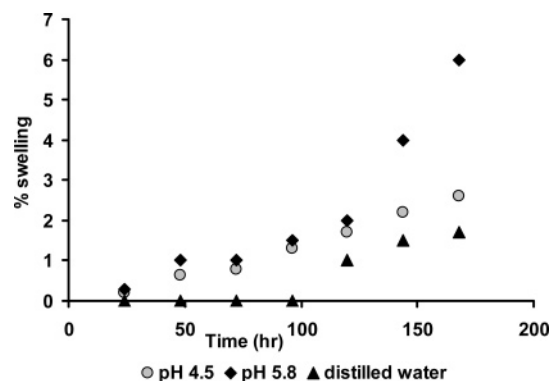


Figure 4. Swelling behavior of NREP films exposed to distilled water, pH 4.5, and pH 5.8.

of 4-VP (11% and 9% w/w) was lowered maintaining the HEMA content at 21% as in P2.

Both polymers P3 and P4 containing a higher percentage of MMA showed very low uptake of water as compared to polymer P2 at pH 4.5 and 5.8, respectively. However, the increase in the content of MMA with reduction in 4-VP as compared to P2 imparted a hydrophobic character. This delayed its dissolution rate, and complete dissolution at pH 1.2 occurred at only 45 min. To enhance the dissolution rate at acidic pH, compositions P5 and P6 containing higher HEMA (37% and 32% w/w, respectively) and lower MMA content (52% and 56% w/w, respectively) than P3 and P4 were synthesized.

As expected, the increase in the content of HEMA in compositions P5 and P6 resulted in rapid dissolution at acidic pH 1.2 as compared to polymers P3 and P4. With an increase in HEMA content, these films showed swelling at pH 4.5 and 5.8 followed by dissolution on day 3 of exposure (Table 3). To ensure inhibition of drug leaching at pH 4.5 and 5.8, enhanced polymer hydrophobicity at this pH was desired. Composition P7 containing 61%, 30%, and 9% w/w of MMA, HEMA, and 4-VP, respectively, was synthesized. The polymer dissolved rapidly (15 min) at pH 1.2. It did not dissolve at pH 4.5 and 5.8 but swelled significantly. Swelling would contribute to diffusional release of the drug, entrapped in the swollen layer, and render the reconstituted suspension bitter over a period of time. To suppress the swelling at pH 4.5 and 5.8, compositions P8 and P9 containing slightly higher MMA (64% and 62%, respectively) and lower HEMA content (24% and 27% w/w) as compared to those of polymer P7 were synthesized. Both P8 and P9 showed rapid dissolution at pH 1.2 and minimal swelling on exposure to buffer pH 4.5 and 5.8 for period of 7 days, as seen in Figures 2 and 3. Thus an optimum polymer composition, which showed minimum swelling at pH 4.5 and above but rapid dissolution at pH 1.2 was arrived at. This composition P9 was taken up for further investigation and is referred as NREP in further discussions.

pH-Dependent Dissolution of NREP. NREP film dissolves completely in the buffer at pH 1.2 in 30–45 min but does not solubilize at pH 4.5 and 5.8. Figure 4 shows equilibrium swelling at pH 4.5 and 5.8 and in distilled water. The comonomer composition influences the response of NREP to different buffers. Poly(4-VP) is a weak base, and solution pH influences its charge.^{27,28} At low pH, ionization of amino groups occurs due to protonation of nitrogen present in the aromatic ring of 4-VP. The presence of 4-VP in NREP facilitates its rapid dissolution at pH 1.2.

The uptake of water by NREP films at pH 4.5 and 5.8 is very low for 2–3 days followed by a slight increase thereafter. The ionization of cationic polymers decreases with an increase

in pH, reducing the hydration and swelling of the polymer.³⁵ At pH 4 the degree of protonation of polyvinyl pyridine is zero and limits its solubility.^{27,28} NREP composition is so optimized that at pH 4.5 4-VP is not protonated and MMA contributes to the hydrophobicity as evident from the very low uptake of water. The swelling of NREP at pH 5.8 was slightly greater than that observed at pH 4.5. Unlike the complete deprotonation of 4-VP at pH 4, significant but incomplete deprotonation of poly(4-VP) occurs at pH 4.8.^{27,28,36} Hence the swelling at pH 5.8 was slightly higher than that observed at pH 4.5. The swelling of NREP in distilled water was negligible (Figures S5 and S6 in the Supporting Information). The dissolution characteristics of NREP make it ideal for the gastric delivery of drugs. The gastric pH is <3,³⁷ and the dissolution pH of NREP is <4. The hydrophobic nature of NREP, rapid dissolution at gastric pH, and insolubility at near neutral pH make NREP an ideal polymer for the formulation of taste-masked products, especially liquid oral preparations such as dry syrup.

Physicochemical and Biological Evaluation of NREP. The molecular weight of NREP determined by gel permeation chromatography (GPC) was found to be 58,550 g/mol, and the polydispersity index was 1.6, indicating a narrow molecular weight distribution. The monomer composition in the polymer was calculated by integration of all protons using NMR spectroscopy. The assignments of the proton signals and the absorption bands for different functional groups in NREP analyzed by NMR and FTIR are discussed in subsequent sections.

In Vitro Biological Reactivity Test. Biocompatibility is a critical consideration in the design and application of biomaterials.³⁰ Evaluation of the in vitro cytotoxicity of a biomaterial is the first step to establish biocompatibility. The response of NREP was compared with the positive control phenol and the negative control ultrahigh molecular weight polyethylene. The extracts of dilute phenol gave severe cytotoxic responses as expected. The L929 cells on treatment with phenol were grainy and lacked normal cytoplasmic space, and large open spaces between the cells indicated cell lysis (data not shown). The negative control elicited no cytotoxic response. The cells were large and confluent and did not show lysis (data not shown). The tests for NREP were conducted in triplicate to ensure accurate judgment. The response of mouse fibroblast cells to NREP extracts is shown in Figure 5. On morphological examination of cell cultures treated with 25% and 50% NREP extract, the cells were confluent and showed discrete intracytoplasmic granules with no cell lysis and without any morphological changes. The absence of loosely bound or detached cells indicated no reactivity toward the cells. The responses for these were graded as “0” indicating no reactivity. The fibroblast cells after contact with 100% NREP extract at an extraction ratio of 0.1 g/mL showed a few loosely attached round cells. The intracytoplasmic granules seen were within acceptable limits as per the USP.²¹ The cultures treated with NREP samples showed that the cells were viable and NREP did not exhibit adverse reactivity.

In Vivo Biological Reactivity Test. None of the animals injected with the NREP extract in a sodium chloride injection and a cottonseed oil for intravenous and intraperitoneal injection tests, respectively, showed any abnormalities or loss in body weight during the observation period. The results showed that NREP extracts in both media meet the requirements of the systemic injection test for intravenous and intraperitoneal applications as per the USP.²¹ The in vitro and in vivo biological reactivity tests show that NREP is nontoxic.

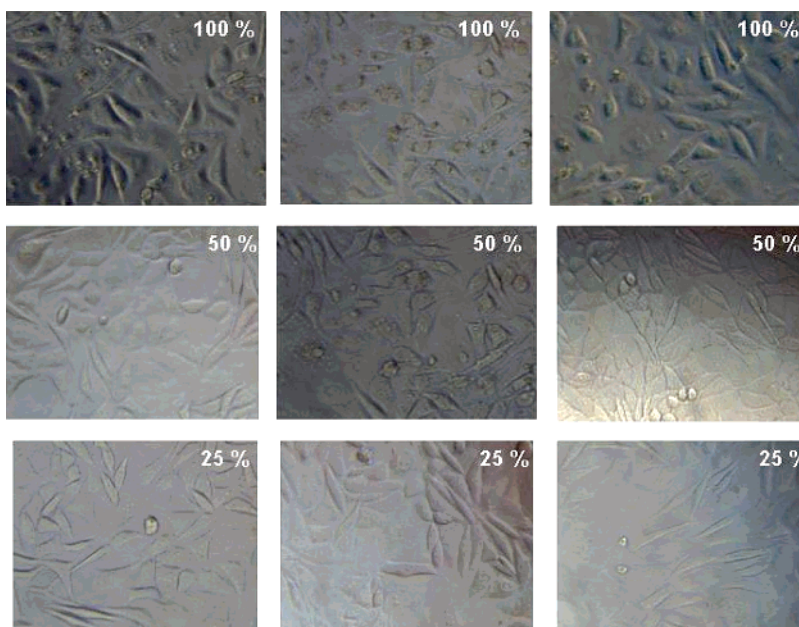


Figure 5. In vitro biological reactivity test on L929 mouse fibroblast cells exposed to 100%, 50%, and 25% extracts of NREP showing confluent cells with discrete intracytoplasmic granules and no cell lysis.

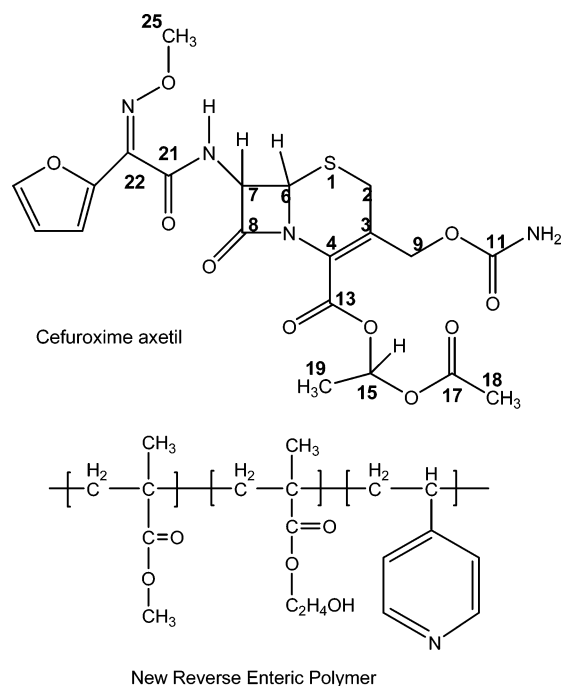


Figure 6. Molecular structures of CA and NREP.

CA–NREP Compatibility Study. Before encapsulation of CA with NREP the interactions between the two were investigated to ensure the retention of CA in its biologically active form. The NMR and FTIR analyses were undertaken to understand the nature of the interactions at a molecular level. The HPLC analysis was undertaken to detect the presence of anti isomers, Δ -2 isomer, cefuroxime, and other impurities. The subsequent sections describe these investigations in detail.

FTIR Spectroscopy. The CA–NREP blends were studied by FTIR analysis and evaluated for the following changes that result from interaction: (1) generation of new bands, (2) hydrogen bonding, (3) band broadening and shifts. The structures and spectra of NREP and CA are shown in Figures 6 and 7, respectively. The peak assignment for CA is as follows:

IR (KBr, cm^{-1}): 3480–3210 (NH, NH_2 complex N–H stretch for primary and secondary amine at C_{11} and C_7

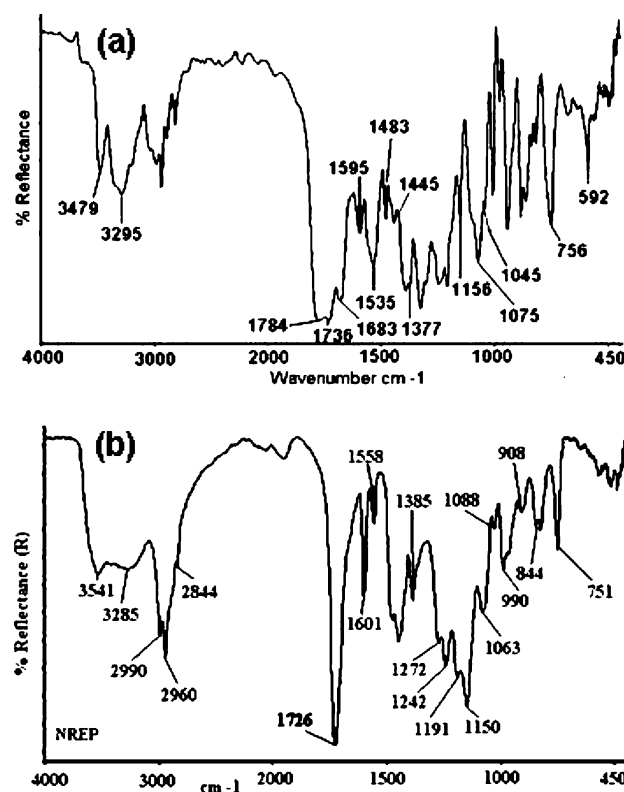


Figure 7. FTIR spectra of (a) CA and (b) NREP in the range of 4000–450 cm^{-1} .

positions); 1783 (β -lactum); 1729 ($\text{C}=\text{O}$, C_{13} , C_{17} positions of CA); 1683 and 1535 (amido, C_7 position of CA); 1729 and 1595 (carbamate, C_9 position of CA); 1075–1010, 1156 ($\text{C}-\text{N}$ stretching, C_{11} , C_{21} positions of CA); 1377 ($\text{C}-\text{N}$ stretching, β -lactum ring); 592 ($\text{S}-\text{C}$, β -lactum ring). These are in agreement with those reported in the literature.^{38–40}

The bands corresponding to β -lactum and carbonyl groups were of significant interest for the CA–NREP interaction study. It has been reported that the conversion of CA to cefuroxime, Δ -2 isomer, and anti isomers leads to deactivation.⁴¹ The conversion of CA to cefuroxime occurs by conversion of the 1-ac-

etoxyethyl ester at the C₁₃ position to carboxylic acid. The C—O, C—O—H, and O—H vibrations are highly characteristic of carboxylic acids. The characteristic bands for the carboxylate functionality are seen in the 1610–1550 cm⁻¹ region. The absence of these in the CA–NREP blend implies the absence of interaction between the two and was confirmed by FTIR analysis.

The peak assignments for NREP are as follows:

IR (KBr, cm⁻¹): 3541 (OH, free OH groups); 1726 (C=O, ester); 2844–2990 (methyl C–H asymmetric/symmetric stretch); 1448–1482 (methyl C–H asymmetric/symmetric bend); 1190–1270 (C–O stretch); 1558–1601, 990 (characteristic of a pyridine ring).

NREP is a terpolymer comprising MMA, HEMA, and 4-VP and contains both proton accepting and donating groups. The carbonyl groups from MMA and HEMA act as proton acceptors and are capable of interacting with the proton donating groups. The nitrogen from the pyridine ring also acts as a proton acceptor and is capable of forming hydrogen bonds. The hydroxyl group of HEMA is a proton donating group. It is expected that such a polymer should exhibit self-association by hydrogen bonding between hydroxyl–carbonyl or hydroxyl–hydroxyl and hydroxyl–pyridine nitrogen groups. The band at 3285 cm⁻¹ in NREP corresponds to a hydrogen-bonded hydroxyl of HEMA comonomer. This band shows a shoulder at 3541 cm⁻¹ corresponding to a free hydroxyl group. The maximum at 3285 cm⁻¹ corresponds to intramolecularly associated hydroxyl groups in NREP.

The band corresponding to a carbonyl from MMA and HEMA in NREP is seen at 1726 cm⁻¹. In addition a shoulder is seen at a lower wave number (1636 cm⁻¹). This indicates the contribution of a carbonyl group of NREP to intramolecular hydrogen bonding. The self-association due to hydrogen bonding between carbonyl and hydroxyls in poly(HEMA) is reported.²⁹ The most intense bands corresponding to pyridine rings are located at 1557, 1597, and 993 cm⁻¹.^{29,42} NREP shows bands corresponding to pyridine at 1601, 1558, and 990 cm⁻¹. The spectrum of NREP shows a shift in the position of the pyridine band at 1597–1601 cm⁻¹, indicating hydrogen bonding between the pyridine nitrogen and the hydroxyls from HEMA, contributing to self-association in the polymer. Similar shifts for hydrogen-bonded pyridine have been reported.^{42,43} Unless self-association between the pyridine nitrogen and the hydroxyl is overcome NREP would not interact with acidic drugs. This self-association would prove helpful in enhancing its compatibility with acidic drugs without their conversion in a salt form. These assumptions were substantiated by our detailed analysis of the CA–NREP blend spectrum.

FTIR Spectra of CA–NREP Blends. The FTIR spectra for the physical mixture and a 50:50 w/w blend of CA and NREP are shown in Figure 8. The IR spectrum for a physical mixture of CA and NREP is additive in nature and exhibits absorption frequencies corresponding to CA and NREP at the respective wave numbers. The spectrum does not show any additional new bands, band broadening, or alteration in frequency, indicating that there is no interaction in the solid state between the two.

The FTIR spectrum of the CA–NREP blend is similar to that of the CA–NREP physical mixture. The bands corresponding to the carbonyl functionality in the ester groups (C₁₃ and C₁₇ positions in the CA structure, Figure 6) are intact, as seen at 1729 cm⁻¹. The band for β -lactum is retained at 1783 cm⁻¹. No new peak corresponding to the carboxylate salt is seen in the 1610–1550 cm⁻¹ region. The spectrum does not show band broadening or shifts characteristic of hydrogen bonding. This leads us to the conclusion that the conversion of CA to cefur-

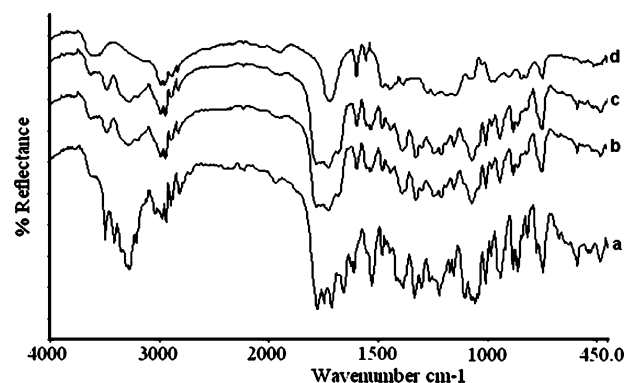


Figure 8. FTIR spectra of (a) CA, (b) physical mixture of CA–NREP, (c) CA–NREP blend, and (d) NREP.

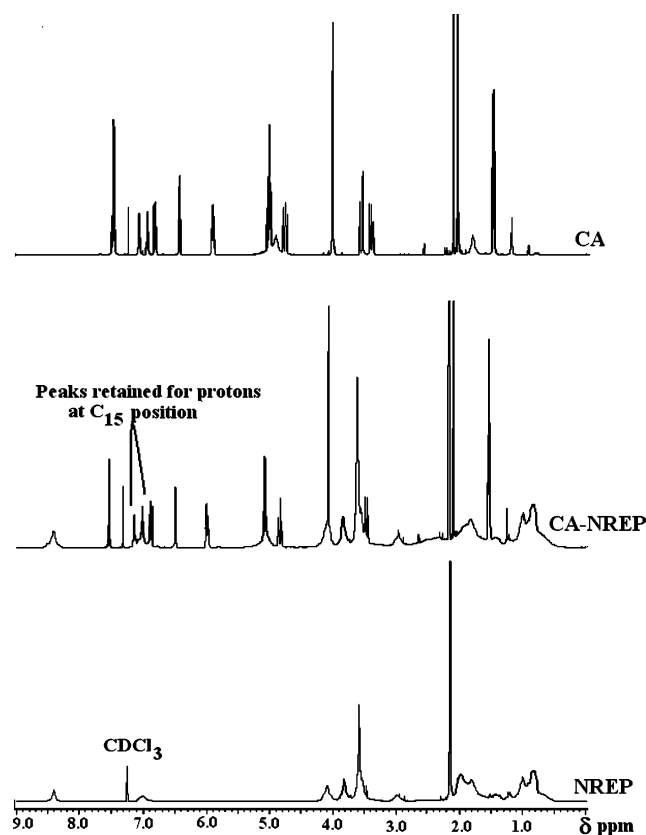


Figure 9. NMR spectra for NREP, CA–NREP blend, and CA. CA is not converted to cefuroxime.

oxime has not taken place in presence of NREP. The bands characteristic of the pyridine group are seen. No new band appears between 1618 and 1637 cm⁻¹, and also bands at 1601 and 1558 cm⁻¹ are present, indicating that the pyridine ring nitrogen is not converted to pyridinium units. This confirms that in the CA–NREP blend pyridine nitrogen is not involved in hydrogen bonding. Our results for non-hydrogen-bonded pyridine are similar to those reported in the past.^{43–45} The FTIR study shows that there is no charge transfer between CA and NREP and CA is physically entrapped in the blend. The absence of bands for carboxylate salt and hydrogen-bonded pyridine confirm this.

¹H NMR Spectroscopy. The ¹H NMR spectrum of the blend was evaluated for the signals corresponding to protons associated with the 1-acetoxyethyl group attached to cefuroxime. The spectra for CA, NREP, and the CA–NREP blend are shown in Figure 9.

^1H NMR of CA. The signals for the CA spectrum are assigned as follows: (CDCl_3 , ppm): 1.5 δ (d, 3H) for CH_3 at the C_{19} position; 2.14 δ (d, 3H) for the $\text{CH}_3\text{--CO--O}$ group at the C_{18} position; 3.45–3.63 δ (dd, 2H) for protons at the C_2 position of the β -lactum; 4.04 δ (s, 3H) for the N--O--CH_3 attached at the C_{22} position; 4.7–4.9 δ (m, 2H) proton at the C_9 position; 5.02–5.04 δ (m, 1H) proton at the C_6 position; 5.04–5.07 δ (m, 1H) proton at the C_9 position; 5.93 δ (m, 1H) proton at the C_7 position; 6.44–6.45 δ (m, 1H) protons in the furan ring; 6.8–6.85 δ (m, 1H) protons in the furan ring; 6.9–7.1 δ (m, 1H) proton at the C_{15} position; 7.47–7.48 δ (d, 1H) protons in the furan ring; 7.5–7.52 δ (d, 1H) proton of the N--H group; signal at 2.07 δ indicates acetone. Yoon et al.³⁹ reported similar assignments for the ^1H NMR of CA.

^1H NMR of NREP. The signals for NREP spectrum are assigned as follows: (CDCl_3 , ppm): 8.43 δ (2H) protons adjacent to the nitrogen of 4-VP in the aromatic ring; 7.03 δ (2H) adjacent to the nitrogen of 4-VP in the aromatic ring; 4.11 δ (2H) protons for the CH_2 group in HEMA; 3.84 δ (2H) protons for the CH_2 group in HEMA; 3.61 δ (3H) protons for OCH_3 ; 2.96 δ (1H) of the CH methine group; 2.01 δ (OH) protons of $\text{C}_2\text{H}_4\text{--OH}$; 1.5–2.0 δ (2H) protons for the CH_2 backbone in the polymer chain; 0.8–1.2 δ (3H) of the CH_3 group; signal at 2.17 δ indicates acetone solvent.

^1H NMR of the CA–NREP Blend. The ^1H NMR for the CA–NREP blend (Figure 9) is additive in nature and shows the presence of signals corresponding to the protons of neat CA and NREP, respectively, indicating the absence of interaction between the two (Figure S7 and Tables S1 and S2 for chemical shifts in the Supporting Information).

The signals corresponding to protons at the C_{15} , C_{18} , and C_{19} positions of the 1-acetoxyethyl group in CA appear in the CA–NREP blend at the same positions as seen in the spectrum of CA. The signal at 2.12 δ (d, 3H) for the $\text{CH}_3\text{--CO--O}$ group at C_{18} position of CA is retained. The signal at 1.5 δ (d, 3H) for CH_3 at the C_{19} position is seen at 1.55 δ . The signals due to the proton at the C_{15} position in CA appear at 6.9–7.1 δ (m, 1H). The spectrum confirms the presence of the 1-acetoxyethyl group in CA in the presence of NREP indicating that CA has not been converted to cefuroxime in the presence of NREP (Figures S7b–d in the Supporting Information). The protons in the furan ring of CA appear as three multiplets at the same position in CA–NREP blend. The signals at 3.45–3.63 δ (dd, 2H), for protons at the C_2 position of the β -lactum ring in CA are merged with the signal for OCH_3 of NREP at 3.6 δ . The signals at 4.06 δ (3H) corresponding to protons of N--O--CH_3 and 5.98 δ for protons at the C_7 position are retained in the CA–NREP blend at the same position as seen in CA spectrum. The signals for the proton at the sixth position of the β -lactum ring and for a proton at the C_9 position appeared at 5.08 δ (1H + 1H) and 4.86 δ (1H) as seen in the spectrum of CA.

The CA–NREP spectrum shows signals for the protons found in the 1-acetoxyethyl group of CA. The ^1H NMR analysis showed that CA is not converted to cefuroxime in presence of NREP. The results of NMR and FTIR analyses are in good agreement and confirm this.

HPLC Analysis. CA exists as a racemic mixture of R and S isomers, and they are resolved by HPLC. The stability and kinetics of degradation of CA have been studied by HPLC in the past. The common degradation products identified are the Δ -2 isomer, cefuroxime, α - and β -sulfoxides, and anti isomers. The CA anti isomers are inactive against β -lactamases.^{41,46–50} The main impurities observed in the presence of polymer CAT

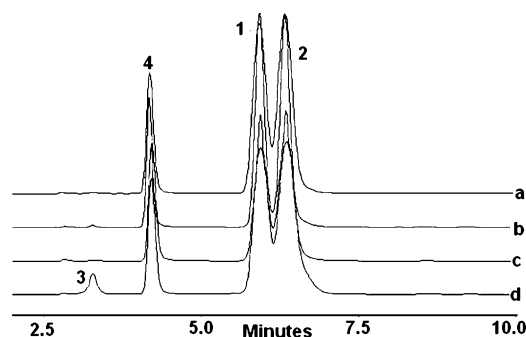


Figure 10. Chromatograms of (a) CA working standard, (b) physical mixture of CA–NREP, (c) CA–NREP blend, (d) CA–NREP blend on aging: (1) isomer B; (2) isomer A; (3) cefuroxime; (4) internal standard acetanilide.

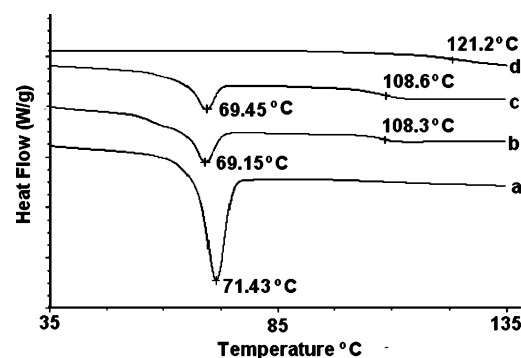


Figure 11. Thermograms of (a) CA, (b) physical mixture of CA–NREP, (c) CA–NREP blend, and (d) NREP.

and EE were cefuroxime, Δ -2 isomer, and β -sulfoxide as described by Cuna et al.¹² and Lorenzo-Lamosa et al.¹³

HPLC Analysis of the CA–NREP Blend. The chromatogram for a CA–NREP physical mixture shows a resolution of 1.63 and a ratio of $r_A/(r_A + r_B)$ is 0.54. The chromatogram shows the absence of the Δ -2 isomer (Figure 10). The cefuroxime content was 0.34%. The other impurity is 0.044%. The total impurities generated are <3% and within the acceptable limits as per the USP.²¹ The results of the CA–NREP blend were identical to those for the physical mixture. CA is stable and does not interact with NREP.

The chromatograms for CA–NREP show that the area for diastereomer B is reduced in presence of NREP but within the acceptable limits as per the USP.²¹ This is seen from the change in the ratio $r_A/(r_A + r_B)$ from 0.52 for neat CA to 0.54 in presence of NREP. Since the ratio has changed, it was necessary to evaluate if this ratio further changes on aging. The blends were therefore analyzed after 6 months. The chromatogram did not show significant deviation from that obtained for the CA–NREP blend after its preparation (2 weeks). The chromatogram showed the absence of Δ -2 isomer impurity. It is therefore evident that CA in the CA–NREP blends is not converted to Δ -2 isomer even after aging for 6 months. The content of cefuroxime in CA–NREP blend on aging was found to be 0.46%. The other impurities generated were less than 1.15×10^{-3} in content. The resolution for the aged sample was 1.64, and the ratio $r_A/(r_A + r_B)$ was maintained to 0.55, which is acceptable as per the USP.²¹ These results indicate that CA is not degraded in the presence of NREP and the ratio of diastereomers A and B is acceptable as per the USP.²¹

DSC Analysis. Thermal analysis of a CA–NREP blend was critical to ensure that CA is retained in the same form in presence of NREP. CA exists in three polymorphic forms.⁵¹ Woo and Chang⁵¹ and Jo et al.⁵² reported that crystalline CA

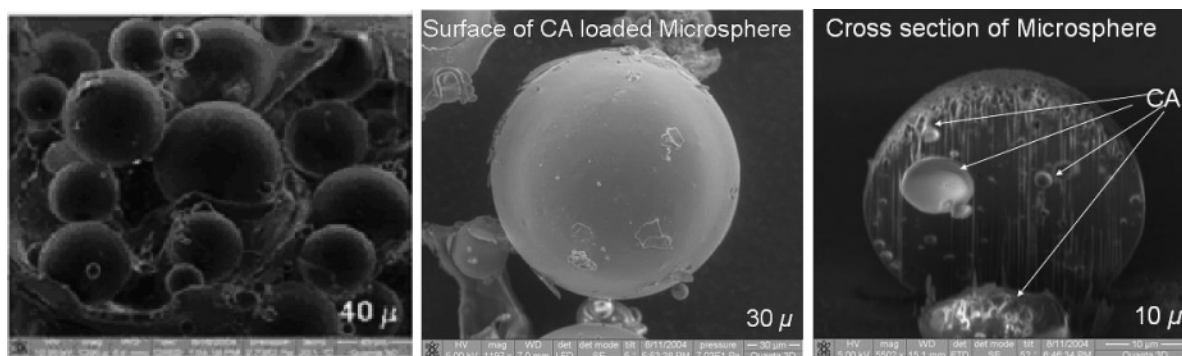


Figure 12. Morphology of CA-loaded microspheres (surface and cross-section of microsphere).

melts at 175–180 °C, and the other two forms melt at 135–137 and 70–80 °C, respectively.

Thermal Behavior of CA. The scan for CA is shown in curve a of Figure 11. The CA sample showed an endotherm at 71.4 °C. These results are in agreement with those reported by Woo and Chang⁵¹ and Woo et al.⁵³

Thermal Behavior of NREP. The T_g for NREP is 121.2 °C (Figure 11, curve d). The monomer composition in random terpolymer NREP was so chosen as to yield a high T_g . The T_g 's of homopolymers of MMA (105 °C), HEMA (87.5 °C), and 4-VP (148 °C) are high.^{43,54} The T_g for the terpolymer is given by Fried⁵⁵ as $T_g = (T_{g1w1} + T_{g2w2} + T_{g3w3})$, where w_1 , w_2 , and w_3 are weight fractions and T_{g1} , T_{g2} , and T_{g3} are the T_g 's of the homopolymers. The experimental T_g value for NREP (121.2 °C) is higher than that arrived at from the above equation (103 °C). This enhancement of T_g over the calculated value is attributed to the intramolecular hydrogen bonding between the hydroxyls from HEMA with the carbonyl of MMA and the nitrogen of 4-VP in NREP as demonstrated by FTIR studies.

The higher T_g obtained for NREP is beneficial in a number of ways. The high T_g of the NREP eliminates the need to store it at lower temperatures and also avoids tackiness during pharmaceutical processes such as drying and heat-sealing involving heat. Increase in T_g as a result of restriction of polymer segment motion due to hydrogen bonding has been reported in the past.^{56–58} It has been reported that intramolecular cross-linking imparts rigid behavior to polymers preventing strong binding with cell membranes thereby reducing cell damage.^{34,59} The increase in T_g of NREP over the weight average value suggests the restricted segmental movement of polymer chains, thus contributing to its restricted interaction with cell membranes and imparting biocompatibility as seen in an earlier section.

Thermal Behavior of CA–NREP Blends. The physical mixture of CA and NREP shows a sharp endotherm at 69.15 °C corresponding to CA (Figure 11, curve b). Thus characteristics of CA are retained in the physical mixture. The CA–NREP blend prepared by evaporation of the solvent shows the endotherm corresponding to CA at 69.45 °C (Figure 11, curve c). The DSC curve for the physical mixture as well as the blend of CA–NREP shows T_g of the polymer at 108 °C. The T_g of NREP is lowered by 15 °C due to its plasticization caused by presence of smaller CA molecules between adjacent polymer segments. Similar results with decreases in polymer T_g in the presence of drug molecules have been reported by Holgado et al.,⁶⁰ Okhamafe and York,⁶¹ and Takka.⁶² The blend does not show a change in the physical form of CA. The above results confirm the absence of drug–polymer interaction in CA and NREP.

Evaluation of NREP for Taste-Masking. The investigation of physicochemical interaction between CA and NREP showed

that CA is not degraded in the presence of NREP. Hence encapsulation of CA by NREP was undertaken and evaluated for taste-masking ability and release at gastric pH. The environmental scanning electron microscopy (ESEM) analysis was used to understand the release mechanism at gastric pH and inhibition of release at salivary pH.

CA Dissolution Studies. The CA loading efficiency in the microspheres was good as seen in Table 2. Figure 12 shows the morphology of the CA microspheres. The cross-section of F1 shows CA dispersed in the matrix. The compendial method for dissolution of CA immediate release tablets describes the use of 0.07 N HCl as a dissolution medium,²¹ and hence the same was chosen to investigate the immediate release of CA. Composition F1 showed rapid dissolution of CA in 0.07 N HCl wherein 78%, 84%, and 87% of CA was released in 30, 60, and 120 min. CA release in 30 min was further enhanced from F2, F3, and F4 compositions, where the NREP loading was lower than that of F1. At the end of 30 and 60 min composition F2 released 80% and 95% of CA, respectively. Compositions F3 and F4 released 86% and 88% of CA after 30 min, respectively, and 90% after 60 min. NREP shows rapid dissolution at acidic pH due to protonation of the tertiary nitrogen from the pyridine ring, and hence variation in polymer loading did not affect the release pattern from these compositions significantly. Further, NREP is insoluble at the pH of saliva; hence it can be used effectively to taste-mask CA without compromising its bioavailability.

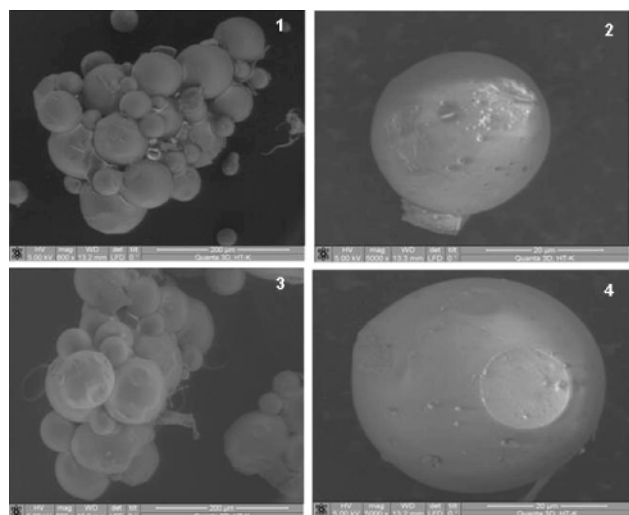
Gustatory Test/Taste Evaluation. For safety and regulatory reasons the minimum loading of synthetic polymers is preferred in oral drug delivery. The daily permissible amount for polymethacrylates is 2 mg/kg body weight,⁶³ and hence compositions F3 and F4 containing lower NREP loading than that in F1 and F2 were considered for taste evaluations. CA exhibits maximum stability at pH 3.5–5.5.⁴⁶ Hence compositions F3 and F4 were reconstituted at pH 4.4 in syrup by adjusting the pH with citric acid–sodium citrate buffer. NREP does not swell at pH 4.5 since the degree of protonation of 4-VP is zero at pH ~4.^{27,28} It was expected that at pH 4.4 compositions F3 and F4 would not release CA, imparting a bitter taste to the syrup. The palatability of the reconstituted suspensions was evaluated on the basis of numerical grading by the volunteers. The mean grading for the reconstituted taste-masked CA microspheres is shown in Table 4. Compositions F3 and F4 retained palatability over 7 days. The volunteers graded the formulations between 0 and 2 and rated the formulations as palatable.

Environmental Scanning Electron Microscopy. Figures 12 and 13 show the morphology of the microspheres before and after suspension in buffer at pH 4.5 and 5.8 for 7 days. The integrity of the polymer film coat at the pH of saliva and also

Table 4. Taste-Masking Test^a

day	1	2	3	4	5	6	7
F3	0	0	0	0	0	1	1
F4	0	0	0	0	1	1	1

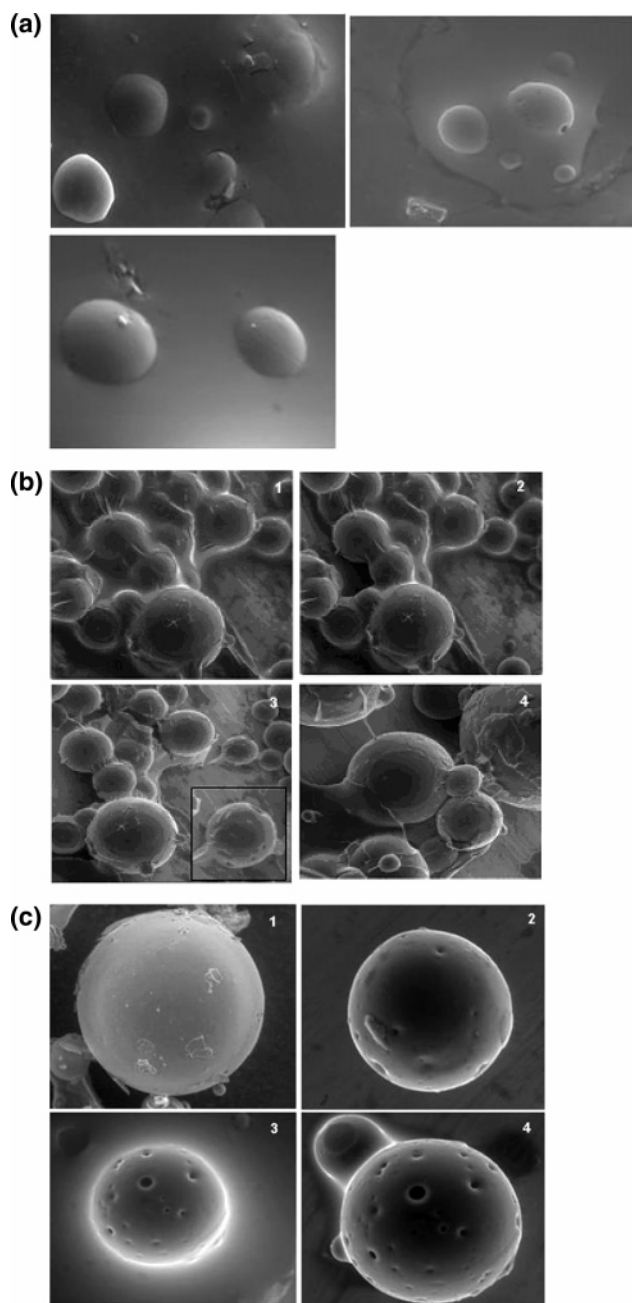
^a 0, sweet; 1, acceptable; 2, acceptable but slightly bitter; 3, bitter; 4, very bitter.

**Figure 13.** Morphological changes in NREP microspheres on exposure to pH 4.5 (1–2) and 5.8 (3–4).

at reconstitution pH 4.5 is crucial to retain the palatability of F3 and F4 formulations. The examination of microspheres recovered from the aqueous medium after 7 days does not show any drastic changes in the morphology. NREP coating on the microspheres remains insoluble and intact as seen in Figure 13. The integrity of the microspheres without any drastic morphological changes is due to the pH-dependent behavior of NREP and its insolubility in water (Figures 4 and 13 and Figure S5 in the Supporting Information). This prevents leaching of CA at the pH of saliva. The morphological changes occurring in 0.07 N HCl were recorded by immersing the microspheres completely in the medium. Extensive changes in the surfaces of the microspheres were observed after immersion in the acid medium. NREP dissolves in the acid, and removal of the acid medium by applying a vacuum resulted in formation of a blanket of polymer film over the microspheres (Figures 14a and 14b). The removal of the film from the surface of the microspheres showed that the smooth surface of the microspheres distorted due to the deposits from the dissolved polymer. An individual microsphere was isolated, drops of 0.07 N HCl were introduced onto it, and the morphological changes were monitored by simultaneous recording. The microsphere developed small craters on exposure to the acid medium after 1–2 min. Figure 14c shows the initiation of pore formation after 5 min. Distinct pores were formed within 10 min. These morphological changes confirm that CA is rapidly released from all compositions (F1–F4) in 0.07 N HCl as a result of polymer dissolution.

Conclusions

Drug–polymer interactions play a critical role in dosage formulation. It has been reported in the past that the interaction of cefuroxime axetil (CA) with other polymers leads to the generation of impurities and inactivation. The investigation of interactions between CA and basic monomers DMAEMA and 4-VP by HPLC revealed that CA was degraded by DMAEMA

**Figure 14.** (a) Morphological changes in microspheres on immersion in buffer pH 1.2. (b) NREP dissolution at pH 1.2 causes a blanket of polymer on removal of buffer (1–2). Microsphere surface is distorted due to deposition of dissolved NREP (3–4). (c) Morphological changes in individual microspheres on exposure to pH 1.2: (1) before exposure; (2) after exposure for 2 min and removal of buffer; (3) after exposure for 5 min still immersed in buffer; (4) formation of pores after removal of buffer in 10 min.

but was stable in presence of 4-VP. A cationic polymer (NREP), containing the hydrophobic monomer MMA, hydrophilic monomer HEMA, and the basic monomer 4-VP, was synthesized. The rationale behind the choice of monomers has been discussed and validated experimentally. The proton donating and accepting groups within NREP resulted in strong self-associations within the polymer. This suppressed the interaction between NREP and CA as revealed by FTIR, NMR, HPLC, and DSC analysis. The composition of NREP was optimized to exhibit rapid dissolution at the acidic pH prevalent in the stomach. The hydrophobicity of the polymer at pH > 4 suppressed CA release from encapsulated particles at the pH of saliva. This masked

the bitter taste of CA without causing inactivation and enhanced palatability as revealed by the gustatory test. The study shows that based on the understanding of intramolecular associations within the polymer and the pharmacokinetics of the drug rapidly releasing palatable granules of CA could be formulated. Further, this study highlights an approach to design new excipients to meet increasingly stringent requirements for stabilization and delivery of difficult to formulate drug molecules.

Acknowledgment. A. Menjoge thanks the Council of Scientific and Industrial Research, New Delhi, India, for financial support. We thank the Shree Chitra Tirunal Institute of Medical Sciences and Technology, Tiruvananthapuram, India, for biological evaluation of the materials.

Supporting Information Available. Procedure for the biological reactivity test, fabrication of the polymer film, pH-dependent dissolution/swelling, instrumentation details for FTIR, DSC, NMR, and HPLC, HPLC method validation, HPLC analysis data for CA–DMAEMA interaction, water uptake study of the NREP film, table for the chemical shifts by ^1H NMR, and NMR spectra for the NREP–CA blend, CA, and the DMAEMA-based polymer–CA blend. This material is available free of charge via the Internet at <http://pubs.acs.org>.

References and Notes

- Langer, R.; Cima, L. G.; Tamada, J. A.; Wintermant, E. *Biomaterials* **1990**, *11*, 738–745.
- Serajuddin, A. M.; Thakur, A. B.; Ghoshal, R. N.; Fakes, M. G.; Ranadive, S. A.; Morris, K. R.; Varia, S. A. *J. Pharm. Sci.* **1999**, *88*, 696–704.
- Mura, P.; Bettinetti, G. P.; Faucci, M. T.; Manderioli, A.; Parrini, P. L. *Thermochim. Acta* **1998**, *321*, 59–65.
- Novoa, G. A. G.; Ki, J. H.; Mirza, S.; Antikainen, O.; Colarte, A. I.; Paz, A. S.; Yliruusi, J. *Eur. J. Pharm. Biopharm.* **2005**, *59*, 343–350.
- Verma, R. K.; Garg, S. J. *Pharm. Biomed. Anal.* **2005**, *38*, 633–644.
- Wissing, S.; Craig, D. Q. M.; Barker, S. A.; Moore, W. D. *Int. J. Pharm.* **2000**, *199*, 141–150.
- Ceschel, G. C.; Badiello, R.; Ronchi, C.; Maffei, P. J. *Pharm. Biomed. Anal.* **2003**, *32*, 1067–1072.
- Mukherji, G.; Goel, S.; Arora, V. K. U. S. Patent 6,565,877, 2003.
- Friend, D. J. *Microencapsulation* **1992**, *9*, 469–480.
- Albertini, B.; Cavallari, C.; Passerini, N.; Voinovich, D.; Gonzalez-Rodriguez, M. L.; Magarotto, L.; Rodriguez, L. *Eur. J. Pharm. Sci.* **2004**, *21*, 295–303.
- Robson, H.; Craig, D.; Deutsch, D. *Int. J. Pharm.* **1999**, *190*, 183–192.
- Cuna, M.; Lorenzo-Lamosa, M.; Vila-Jato, J.; Torres, D.; Alonso, M. *Drug Dev. Ind. Pharm.* **1997**, *23*, 259–265.
- Lorenzo-Lamosa, M.; Cuna, M.; Vila-Jato, J.; Torres, D.; Alonso, M. *J. Microencapsulation* **1997**, *14*, 607–616.
- Donn, K.; James, N.; Powell, J. J. *Pharm. Sci.* **1994**, *83*, 842–844.
- Dantzig, A. H.; Dale, C.; Duckworth, L.; Tabas, B. *Biochim. Biophys. Acta* **1994**, *1191*, 7–13.
- Campbell, C.; Chantrell, L.; Eastmond, R. *Biochem. Pharmacol.* **1987**, *36*, 2317–2324.
- Ruiz-Balaguer, N.; Nacher, A.; Casabo, V.; Merino, M. *Antimicrob. Agents Chemother.* **1997**, *41*, 445–448.
- In *Physicians' Desk Reference*; 56th Ed.; 2002, pp 1892–1902; Medica Economics Company Inc.: Montvale, New Jersey.
- Finn, A.; Straughn, A.; Meyer, M.; Chubb, J. *Biopharm. Drug Dispos.* **1987**, *8*, 519–526.
- Deutsch, D. S.; Anwar, J. U. S. Patent 4,897,270, 1990.
- USP 26–NF 21*; United States Pharmacopoeia: Rockville, MD, 2003.
- Kulkarni, M. G.; Menjoge, A. R. U. S. Patent 20050137372 A1, 2005.
- Kulkarni, M. G.; Menjoge, A. R. U. S. Patent 20050136114 A1, 2005.
- Park, J.; Lim, Y.; Kwon, Y.; Jeong, B.; Choi, Y.; Kim, S. *J. Polym. Sci., Part A: Polym. Chem.* **1999**, *37*, 2305–2309.
- Functional Monomers; Their Preparation, Polymerization, and Application*; Yocum, R. H.; Nyquist, E. B., Eds.; Marcel Dekker: New York, 1974; Vol. 2.
- Tomme, S.; Steenbergen, M.; Smedt, S.; Nostrum, C.; Hennink, W. *Biomaterials* **2005**, *26*, 2129–2135.
- Radeva, T.; Milkova, V.; Petkanchin, I. *J. Colloid Interface Sci.* **2004**, *279*, 351–356.
- Pefferkorn, E.; Elaissari, A. *J. Colloid Interface Sci.* **1990**, *138*, 187–194.
- Cesteros, L. C.; Meaurio, E.; Katime, I. *Macromolecules* **1993**, *26*, 2323–2330.
- Wang, Y.; Robertson, J.; Spillman, W.; Claus, R. *Pharm. Res.* **2004**, *21*, 1362–1373.
- Agarwala, R.; Unferb, S.; Mallapragada, K. *J. Controlled Release* **2005**, *103*, 245–258.
- Mao, S.; Shua, X.; Unger, F.; Wittmar, M.; Xie, X.; Kissel, T. *Biomaterials* **2005**, *26*, 6343–6356.
- Bruining, M.; Blaauwgeers, H.; Kuijter, R.; Pels, E.; Nuijts, R.; Koole, L. *Biomaterials* **2000**, *21*, 595–604.
- Fischer, D.; Ahlemeyer, Y.; Krieglstein, J.; Kissel, T. *Biomaterials* **2003**, *24*, 1121–1131.
- Said, A. *Biomaterials* **2005**, *26*, 2733–2739.
- Prochazka, K.; Martin, T.; Munk, P.; Webber, S. *Macromolecules* **1996**, *29*, 6518–6525.
- Qiu, Y.; Park, K. *Adv. Drug Delivery Rev.* **2001**, *53*, 321–339.
- Crisp, H. A.; Clayton, J. C. U. S. Patent 4,820,833, 1989.
- Yoon, G.; Jeong, H. S.; Yim, S. S. PCT Application WO 09843980A1, 1998.
- Hwang, T. S.; Ahn, C. Y. PCT Application WO 00216372 A1, 2002.
- Fabre, H.; Bork, H. I.; Lerner, D. A. *J. Pharm. Sci.* **1994**, *83*, 553–558.
- Cesteros, L.; Velada, J.; Katime, L. *Polymer* **1995**, *36*, 3183–3189.
- Ruokolainen, J.; Brinke, G.; Ikkala, O. *Macromolecules* **1996**, *29*, 3409–3415.
- Yarapathi, R. V.; Reddy, S. M.; Tammishetti, S. *React. Funct. Polym.* **2005**, *64*, 157–161.
- Goh, S. H.; Lee, S. Y.; Zhou, X.; Tan, K. L. *Macromolecules* **1998**, *31*, 4260–4264.
- Nguyen, N. T. *Pharm. Res.* **1991**, *81*, 893–898.
- Tejchman, B.; Jarominska, M.; Horodecka, M.; Oszczapowicz, I. *Acta Pol. Pharm.* **1995**, *52*, 477–482.
- Tejchman, B.; Oszczapowicz, I. *Acta Pol. Pharm.* **1997**, *54*, 7–12.
- Zajac, M.; Jelinska, A.; Dobrowolski, L.; Oszczapowicz, I. *J. Pharm. Biomed. Anal.* **2003**, *32*, 1181–1187.
- Zivanovic, L.; Ivanovic, I.; Vladimirov, S.; Zecevic, M. *J. Chromatogr., B: Biomed. Sci. Appl.* **2004**, *800*, 175–179.
- Woo, J. S.; Chang, H. C. U. S. Patent 6,107,290, 2000.
- Jo, G. H.; Yu, J. H.; Yun, J. H.; Hwang, S. J.; Woo, J. S. Preparation of amorphous form of cefuroxime axetil using supercritical fluid processing. In *Controlled Release Society 29th Annual Meeting Proceedings*, Seoul, South Korea, July 20–25, 2002; Abstract 057.
- Woo, J. S.; Chang, H. C.; Lee, C. H. *J. Korean Pharm. Sci.* **2002**, *32*, 73–80.
- Peyser, P. In *Polymer Handbook*, 3rd ed.; Brandup, J., Immergut, E. H., Eds.; Wiley: New York, 1989; pp 209–277.
- Fried, J. R. *Polymer Science and Technology*; Prentice Hall: New Delhi, India, 1999; pp 132–164.
- Schneider, H. A. Glass Transition (Theoretical Aspects). In *Polymeric Materials Encyclopedia*, CD-ROM version; Salamone J. C., Ed.; CRC Press: Boca Raton, FL, 1996.
- Jiang, M.; Li, M.; Xiang, M.; Zhou, H. *Adv. Polym. Sci.* **1999**, *146*, 121–196.
- Mayo-Pedrosa, M.; Alvarez-Lorenzo, C.; Concheiro, A. *J. Therm. Anal. Calorim.* **2004**, *77*, 681–693.
- Gebhart, C.; Kabanov, A. *J. Controlled Release* **2001**, *73*, 401–416.
- Holgado, M. A.; Arevalo, M. A.; Fuentes, J. A.; Caraballo, I.; Llera, J. M.; Rabasco, A. M. *Int. J. Pharm.* **1995**, *114*, 13–21.
- Okhamafe, A. O.; York, P. J. *Pharm. Pharmacol.* **1989**, *41*, 1–6.
- Takka, S. *Farmaco* **2003**, *58*, 1051–1056.
- Handbook of Pharmaceutical Excipients*, 3rd ed.; Kibbe, A. H., Ed.; American Pharmaceutical Association: Washington, DC, 2000.

BM060673V